

Supplementary Information

Immobilization of molecular complexes on graphitized carbon cloth as stable and hybrid electrocatalysts for enhanced Hydrogen evolution reaction and Oxygen evolution reaction

Ram Murthy^a, Chittor Neelakantan Sundaresan^{a}*

^aDepartment of chemistry, Sri Sathya Sai Institute of Higher Learning, Brindavan Campus, Kadugodi, Bengaluru – 560067, India

Table of Contents

- 1. Instrumentation**
- 2. Synthesis**
- 3. Characterization**
- 4. Electrode preparation and electrochemical measurements**
- 5. X-ray Photoelectron Spectroscopy (XPS)**
- 6. UV-Vis Spectroscopic Analysis**
- 7. Vibrating Sample Magnetometer**
- 8. Thermogravimetric Analysis**
- 9. Proposed Mechanism of Hydrogen Evolution Reaction (HER)**

S1. Instrumentation

The solvents used in the study were of analytical grade and were used without further purification. Milli-Q water was used throughout the study to prepare electrolyte solutions. H₂SO₄ (98 %) and KOH (AR) were brought from Merck chemicals. The metal salts were procured from Merck chemicals. Fourier transform-infrared spectroscopy (FTIR) measurements were performed on L1600300 Spectrum TWO Perkin-Elmer FTIR spectrum instrument within the range of 400-4000 cm⁻¹. Bruker Ascend 400 MHz with DMSO-d₆ as solvent was used to obtain ¹H and ¹³C NMR spectra of the complexes. Mass spectroscopy (MS) data was obtained using GCMS-QP2010 Shimadzu equipment. Scanning electron microscopy (SEM) images of the samples were acquired on JEOL model JSM-IT 300 electron microscope. Magnetic spectra of the complexes were obtained with vibrating sample magnetometer on MODEL FCM-10 Magnetic field control module. The electrochemical measurements were carried out using VSP-300 BioLogic bipotentiostat instrument for evaluating electrochemical activities of the synthesized complexes towards hydrogen evolution reaction (HER) and oxygen evolution reaction (OER).

S2. Synthesis

The procedure for preparation of ligand has been described in detail in an earlier publication¹. To the appropriate metal chloride (1 mmol) in ethanol and water mixture (1:1, 25mL) at 60 °C was added 2-thioureidobenzothiazole (0.41 g, 2 mmol) and refluxed for 2 hr under constant stirring. The reaction mixture was then cooled and the complex formed was filtered, washed twice with a 1:1 ethanol:water mixture and dried under vacuum for an hour¹.

S3. Characterization

S3.1.¹ Ligand 1-(benzo [d] thiazol-2-yl) thiourea (BTT)

2-thioureidobenzothiazole (BTT): Yellow solid, Yield: 80%, M.p.: 174 °C

UV-Vis: λ_{max} (DMSO): 306 nm.

IR (KBr): 3180, (–N–H stretching), 3017 (–N–H stretching), 1611 (N–H bend), 1030 (C–C stretching), 1184 (–C=S stretching) and 750 cm⁻¹ (ortho-disubstituted), 658(N-H wag).

$^1\text{H-NMR}$ (DMSO- d_6): δ 2.54 (s, 1H, NH), δ 9.30 (s, 2H, NH_2), δ 7.27-7.85 (m, 4H, Aromatic).

$^{13}\text{C-NMR}$ (DMSO- d_6): δ 181.36 ($-\text{C}=\text{S}$), δ 161.66 ($-\text{C}=\text{N}$), δ 136.2, 132.1, 130.57, 126.76, 124.28, 122.1 ($-\text{C}=\text{C}$), δ 40.31 ($\text{C}-\text{NH}_2$).

Mass m/z (% abundance): 209 (35), 175 (25), 159 (100), 96 (41), 83(22), 57 (60)¹.

S3.2. Pd(BTT)₂Cl₂

Pd(BTT)₂Cl₂: Reddish brown solid, yield: 40%. M.p.: 238 °C

Analysis: calculated (%): C₁₆H₁₂Cl₂PdN₆S₄: C, 32.86, H, 2.32, N, 14.1, S, 21.57.

Found (%): C, 30.86, H, 2.87, N, 14.1, S, 21.87.

UV-Vis: λ_{max} (DMSO): 290 nm, 356 nm.

IR data: 3478 ($-\text{N}-\text{H}$ stretching), 3279 ($-\text{N}-\text{H}$ stretching), 2959 ($-\text{C}-\text{H}$ stretching), 1132 ($-\text{C}=\text{S}$ stretching), 1629 ($\text{N}-\text{H}$ bend), 1585 (thioamide stretching), 1310 ($-\text{C}-\text{N}$ stretching), 706 (thioamide bending), 755 (1,2 disubstituted).

$^1\text{H-NMR}$ (DMSO- d_6): δ 12.36 (2H, s NH_2), δ 7.40-7.82 (4H, m, Aromatic).

$^{13}\text{C-NMR}$ (DMSO- d_6): δ 176.5, 175.2, 163.4, 163.1 ($-\text{C}=\text{N}$), δ 147.46, 147.46 ($-\text{C}-\text{S}$), δ 115.9- 138.7 ($-\text{C}=\text{C}$).

S3.3.¹ [Co(BTT)₂Cl₂]

[Co(BTT)₂Cl₂]: Reddish-brown solid, Yield: 79%, M.p.: 320 °C

UV-Vis: λ_{max} (DMSO): 290 nm, 356 nm.

IR data: 3012 ($-\text{N}-\text{H}$ stretching), 1184 ($-\text{C}=\text{S}$ stretching), 1611 ($\text{N}-\text{H}$ bend), 1585 (thioamide stretching), 1310 ($-\text{C}-\text{N}$ stretching), 786 (thioamide bending), 750 (1,2 disubstituted).

$^1\text{H-NMR}$ (DMSO- d_6 ; δ 9.07 (2H, d, NH_2), δ 7.40-7.82 (4H, m, Aromatic).

$^{13}\text{C-NMR}$ (DMSO- d_6): δ 172.63, 171.18 ($-\text{C}=\text{N}$), δ 154.21 ($-\text{C}-\text{S}$), δ 110.39-139.53 ($-\text{C}=\text{C}$).

S3.4.¹ [Ni(BTT)₂Cl₂]

[Ni(BTT)₂Cl₂]: Pale green solid, Yield: 82%, M.p.: 284 °C

UV-Vis: λ_{max} (DMSO): 290 nm, 356 nm.

IR data; 3001 ($-\text{N}-\text{H}$ stretching), 2695 ($-\text{C}-\text{H}$ stretching), 1623($\text{N}-\text{H}$ bend), 1302 ($-\text{C}-\text{N}$ stretching), 996($-\text{C}=\text{S}$ stretching), 1508 (thioamide stretching), 740 (thioamide bending), 743 (1,2 disubstituted).

$^1\text{H-NMR}$ (DMSO- d_6); δ 9.71 (2H, d, NH_2), δ 7 -7.32 (4H, m, Aromatic).

$^{13}\text{C-NMR}$ (DMSO- d_6); δ 170.9, 171.8, 171.14, 172.74 ($-\text{C}=\text{N}$), δ 148.0, 147.7($-\text{C}-\text{S}$), δ 117.94 -129.72 ($-\text{C}=\text{C}$).

S4. Electrode preparation and electrochemical measurements

The working electrode (WE) was prepared by using 1.8 mg of electroactive material, dispersed ultrasonically in a mixture containing 0.70 ml of water and 0.3 ml of isopropyl alcohol (IPA). Further, 0.2 mg of conducting carbon and 10 μl of 5 wt.% Nafion solution was added to the mixture to obtain homogenous ink of the catalyst. Subsequently 10 μl of the electroactive material was drop casted on to a precleaned glassy-carbon electrode (GCE) with diameter 3 mm diameter resulting in a catalyst loading of 0.282 mg cm^{-2} . The modified GCE was dried under room temperature conditions and was used as working electrode.

Electrochemical measurements were performed using conventional three electrode system comprising of glassy carbon electrode (GCE) as working electrode (WE), graphite rod as counter electrode (CE) and saturated calomel electrode (SCE) as the reference electrode (RE) for Hydrogen evolution reaction (HER) and mercury/mercury oxide as reference electrode (RE) for oxygen evolution reaction (OER). Linear sweep voltammograms (LSV) were recorded in potentiodynamic mode. The electrolyte consisting of 0.5 M H_2SO_4 was de-aerated using N_2 gas for a period of 30 minutes.

The measured potential vs SCE and Hg/HgO were normalized with respect to RHE (reversible hydrogen electrode) using the relation $E_{\text{RHE}}=E^\circ + 0.059 \text{ pH} + E_{\text{RHE}}$ and $E_{\text{RHE}}=E^\circ + 0.098 + 0.059\text{pH}$ respectively. Current which resulted from LSV technique was normalized with the geometrical area of the glassy carbon electrode (WE) (0.071 cm^2). Linear sweep voltammetry (LSV) and cyclic voltammetry (CV) were recorded in 0.5 M H_2SO_4 / 0.1 M KOH at a scan rate of 50 mV s^{-1} in N_2/O_2 saturated electrolytes. Cyclic voltammograms (CV) were recorded at various scan rates (20 - 200 mV s^{-1}) to determine capacitance double layer value and the electrochemical active surface area (ECSA).

Sl. No	Electrocatalyst	Electrolyte	Overpotential (mV)	Tafel slope (mV dec ⁻¹)	Reference
1	NiSe ₂ @NG	0.5 M H ₂ SO ₄	248	74.2	2
2	Mo ₂ C-GNR's	0.5 M H ₂ SO ₄	167	74	3
3	Fe ₂ P @NC	0.5 M H ₂ SO ₄	138	97	4
4	MoS ₂ /G-HS	0.5 M H ₂ SO ₄	180	79	5
5	CoS _x @MoS ₂	0.5 M H ₂ SO ₄	239	103	6
6	Ni @CNT's	0.5 M H ₂ SO ₄	261	88	7
7	Pd (II) BTT	0.5 M H ₂ SO ₄	178	73.74	Present work

Table 1 Comparison of HER activity of M (II) BTT with those of existing transition metal based electrocatalyst in 0.5 M H₂SO₄.

Sl. No	Electrocatalyst	Electrolyte	Overpotential (mV)	Tafel slope (mV dec ⁻¹)	Reference
1	Co doped Cu ₇ S ₄	0.1 M KOH	270	130	8
2	Fe-Co-P alloy	0.1 M KOH	252	33	9
3	Ag @Co _x P	0.1 M KOH	310	76.4	10
4	NiO/NiCo ₂ O ₄	0.1 M KOH	430	49	11
5	NiFe.LDH	0.1 M KOH	243	50	12
6	3D NiCoSe ₂ /NF	0.1 M KOH	183	88	13
7	Ni (II) BTT	0.1 M KOH	250	93	Present work

Table 2 Comparison of OER catalytic activity of M (II) BTT complexes with those of existing transition metal based electrocatalyst.

S5. X-ray Photoelectron Spectroscopy (XPS)

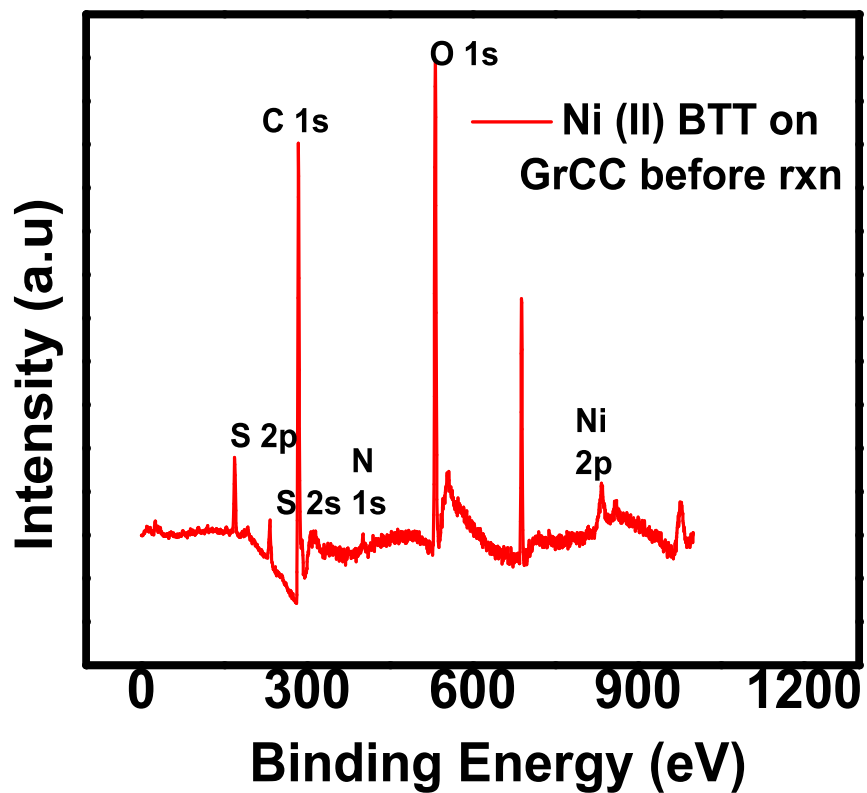


Figure: S1. XPS spectrum of Ni (II) BTT on graphitized carbon cloth prior to the reaction.

S6. UV-Vis Spectroscopic Analysis

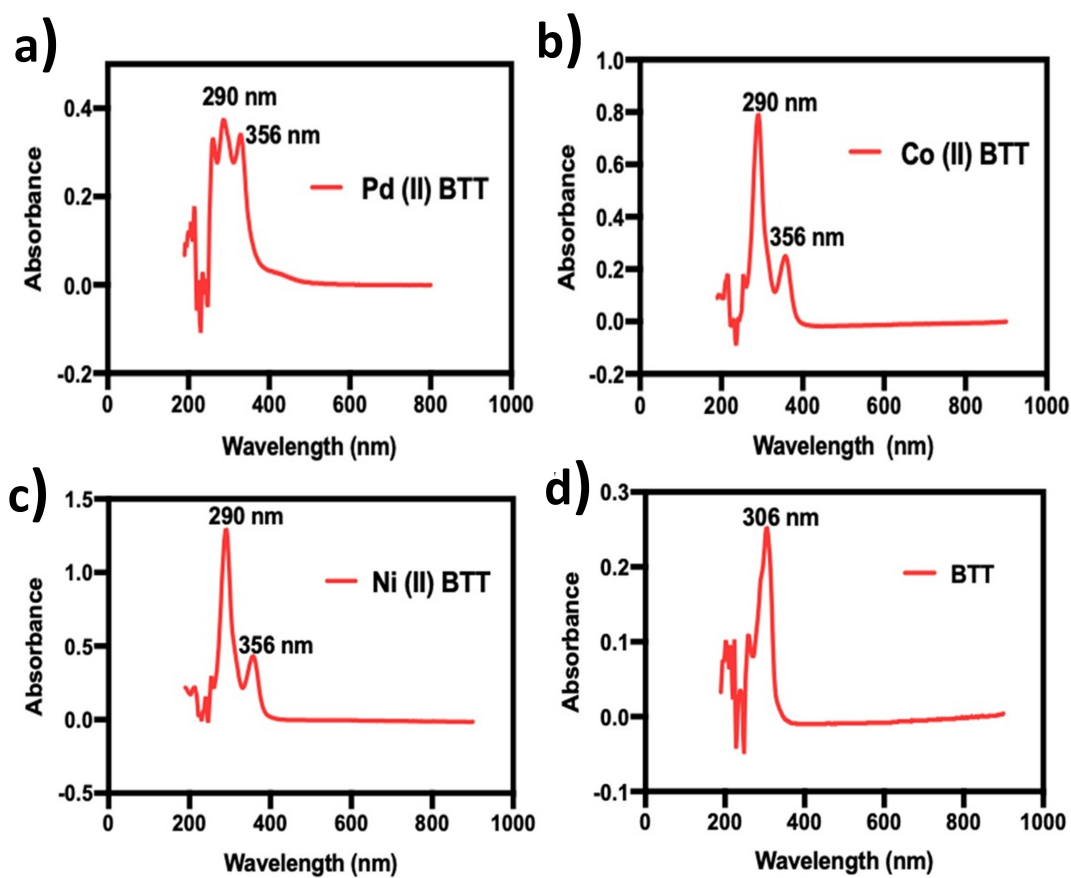


Figure: S2. UV-Vis spectrum of metal complexes a) Pd (II) BTT b) Co (II) BTT c) Ni (II) BTT and 2-thioureidobenzothiazole ligand.

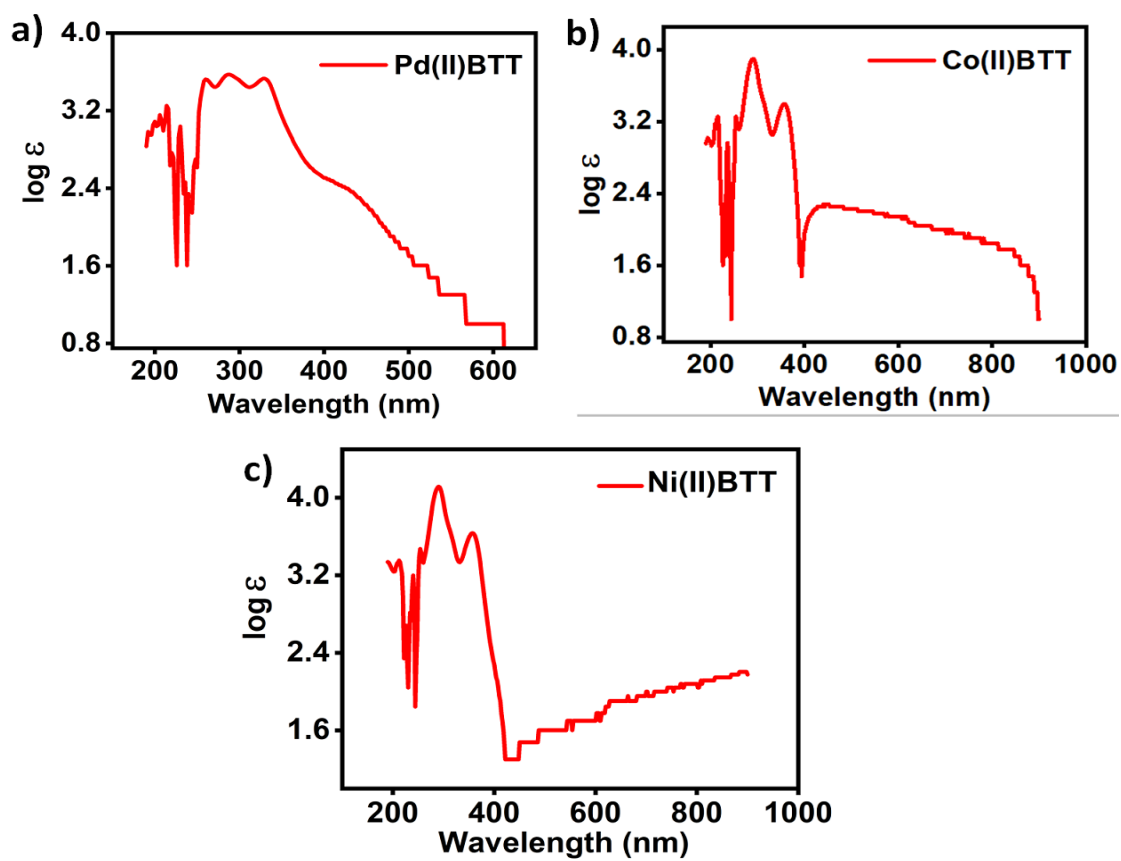


Figure: S3. The graph of $\log \epsilon$ vs Wavelength of metal complexes a) Pd (II) BTT b) Co (II) BTT c) Ni (II) BTT

S7. Vibrating Sample Magnetometer (VSM)

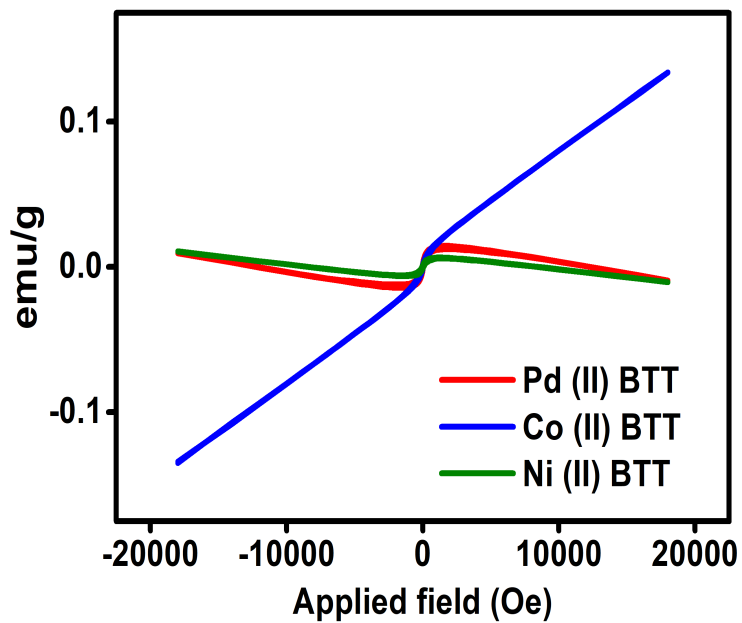


Figure: S4. VSM spectra of M(II)BTT complexes (Pd, Co and Ni).

S8. Thermogravimetric Analysis (TGA)

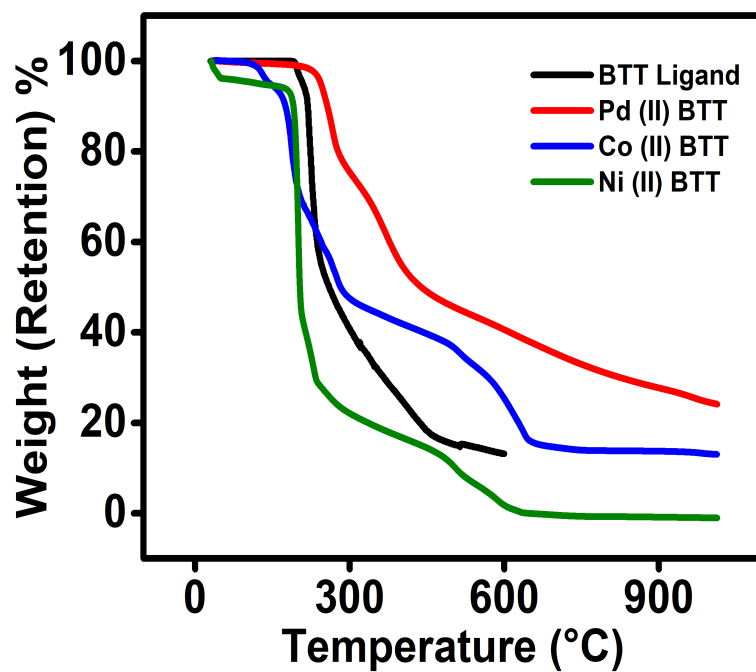


Figure: S5. TGA spectra of M (II) BTT complexes (Pd, Co and Ni).

S9. Proposed Mechanism of Hydrogen Evolution Reaction (HER)

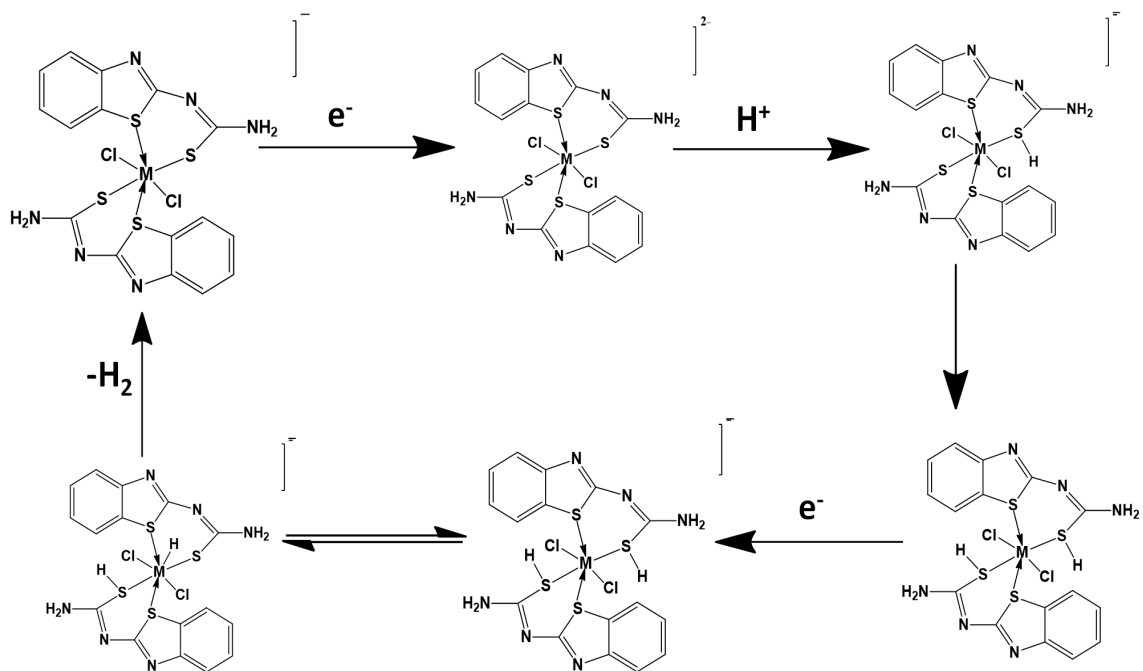


Figure: S6. Proposed proton coupled electron transfer (PCET) HER mechanism catalyzed by 2-thioureidobenzothiazole metal complexes in acidic conditions.

references

- [1] H. Yapati, S. R. Devineni, S. Chirumamilla and S. Kalluru, *Journal of Chemical Sciences*, 2016, **128**, 43–51.
- [2] L. Ai, J. Su, M. Wang and J. Jiang, *ACS Sustainable Chemistry & Engineering*, 2018, **6**, 9912–9920.
- [3] W. Gao, Y. Shi, Y. Zhang, L. Zuo, H. Lu, Y. Huang, W. Fan and T. Liu, *ACS Sustainable Chemistry & Engineering*, 2016, **4**, 6313–6321.
- [4] Z. Pu, C. Zhang, I. S. Amiin, W. Li, L. Wu and S. Mu, *ACS Applied Materials & Interfaces*, 2017, **9**, 16187–16193.
- [5] X. Yu, G. Zhao, S. Gong, C. Liu, C. Wu, P. Lyu, G. Maurin and N. Zhang, *ACS Applied Materials & Interfaces*, 2020, **12**, 24777–24785.
- [6] L. Yang, L. Zhang, G. Xu, X. Ma, W. Wang, H. Song and D. Jia, *ACS Sustainable Chemistry & Engineering*, 2018, **6**, 12961–12968.
- [7] B. Thangavel, S. Berchmans and G. Venkatachalam, *Energy & Fuels*, 2020, **35**, 1866–1873.
- [8] Q. Li, X. Wang, K. Tang, M. Wang, C. Wang and C. Yan, *ACS nano*, 2017, **11**, 12230–12239.
- [9] K. Liu, C. Zhang, Y. Sun, G. Zhang, X. Shen, F. Zou, H. Zhang, Z. Wu, E. C. Wegener, C. J. Taubert *et al.*, *Acs Nano*, 2018, **12**, 158–167.
- [10] Y. Hou, Y. Liu, R. Gao, Q. Li, H. Guo, A. Goswami, R. Zboril, M. B. Gawande and X. Zou, *ACS Catalysis*, 2017, **7**, 7038–7042.
- [11] Y. Wang, Z. Zhang, X. Liu, F. Ding, P. Zou, X. Wang, Q. Zhao and H. Rao, *ACS Sustainable Chemistry & Engineering*, 2018, **6**, 12511–12521.
- [12] C. Wu, H. Li, Z. Xia, X. Zhang, R. Deng, S. Wang and G. Sun, *ACS Catalysis*, 2020, **10**, 11127–11135.
- [13] K. Akbar, J. H. Jeon, M. Kim, J. Jeong, Y. Yi and S.-H. Chun, *ACS Sustainable Chemistry & Engineering*, 2018, **6**, 7735–7742.